

Giant magnetocaloric effect in the Ising antiferromagnet DySb

W. J. Hu,^{a)} J. Du, B. Li, Q. Zhang, and Z. D. Zhang

Shenyang National Laboratory for Materials Science, Institute of Metal Research and International Centre for Materials Physics, Chinese Academy of Sciences, 72 Wenhua Road, Shenyang 110016, People's Republic of China

(Received 20 February 2008; accepted 24 April 2008; published online 13 May 2008)

The magnetic phase transitions and the magnetocaloric effect in the Ising antiferromagnet DySb have been studied. A field-induced sign change of the magnetocaloric effect has been observed which is related to a first-order field-induced metamagnetic transition from the antiferromagnetic to the ferromagnetic states at/below the Néel temperature T_N , while the negative field-induced entropy change is found to be associated with the first-order magnetic transition from the paramagnetic to the ferromagnetic states above T_N . The large magnetic-entropy change (-20.6 J/kg K at 11 K for a field change of 7 T), together with small hysteresis, suggests that DySb could be a potential material for magnetic refrigeration in the low-temperature range. © 2008 American Institute of Physics. [DOI: 10.1063/1.2928233]

Magnetic refrigeration based on the magnetocaloric effect (MCE) has attracted much interest due to its energy-efficient and environment-friendly features, compared with the common gas-compression refrigeration technology.¹⁻³ Until now, the MCE has only been applied in practice in magnetic-refrigeration devices in the low-temperature range ($T < 20$ K) by using the paramagnetic (PM) salt $Gd_3Ga_5O_{12}$.⁴ Therefore, from the point of view of application, it is desirable to explore magnetocaloric materials applicable in different temperature ranges. Recently, however, most interest is focused on possible applications at room temperature. Usually, a large MCE is obtained near the magnetic-ordering temperature T_C of a ferromagnet, because an external magnetic field most effectively affects the order of the spins at or near T_C . A giant MCE (GMCE) is often related with a first-order magnetic transition (FOMT). Typical examples are ferromagnetic (FM) materials $Gd_5(Ge_{1-x}Si_x)_4$,⁵ $La(Fe_{1-x}Si_x)_{13}$,⁶ $MnAs_{1-x}Sb_x$,⁷ $MnFeP_{0.45}As_{0.55}$,⁸ and $MnAs$,⁹ where a negative magnetic-entropy change (ΔS_M) is observed near the FOMT from PM to FM states. The FM shape memory alloys¹⁰⁻¹² also show the GMCE near the martensite transition due to the large difference in magnetic behavior between the martensite and austenite phases. However, usually, in these FM materials the FOMT is accompanied by a huge field or temperature hysteresis which is disadvantageous for applying them in magnetic refrigeration. Consequently, it is necessary to explore new kinds of materials with a large MCE and, also, a small hysteresis. Recently, a GMCE has been found in antiferromagnetic (AFM) systems, such as ϵ - $(Mn_{0.83}Fe_{0.17})_{3.25}Ge$ (Ref. 13) [or $ErRu_2Si_2$ (Ref. 14)], where the large MCE is ascribed to a field-induced metamagnetic transition from a collinear AFM to a triangular AFM (or from AFM to FM) states. Compared with the FM GMCE materials, the thermal or magnetic hysteresis in the AFM systems is quite small, which makes them more suitable for industrial application from the aspect of refrigerant efficiency and energy conservation. In this letter, we present the magnetic and magnetocaloric properties of the Ising antiferromagnet DySb.¹⁵ In this compound, we have observed a

field-induced MCE conversion (i.e., the MCE changes its sign in the applied magnetic field) and a giant negative (conventional) magnetic-entropy change.

Polycrystalline DySb was prepared by direct reaction of elements Dy (99.9%) and Sb (99.999%) in an evacuated silica tube at 600 °C for 3 days. An excess of Sb (4 wt %) was added to compensate the weight loss during annealing. X-ray diffraction pattern confirms the single-phase state of the prepared compound, which crystallizes in the face-centered cubic NaCl type of structure. The lattice parameter was determined to be 6.161 Å using the Rietveld refinement method. The magnetic properties were measured in a superconducting quantum interference device magnetometer from 5 to 300 K and in applied magnetic fields up to 7 T. The temperature dependence of the magnetization was recorded in a magnetic field of 0.005 T upon heating after zero-field cooling.

DySb undergoes a PM-AFM transition at its Néel temperature $T_N \sim 9$ K, as shown in Fig. 1. The compound is a typical Ising antiferromagnet in which the FM sheets are antiferromagnetically stacked along the $\langle 111 \rangle$ direction and the moments are collinear with the $[001]$ axis (Ising axis).¹⁶ It has been reported that there are two metamagnetic transitions at about 2.4 and 4.8 T along the $[001]$ direction and one at about 2.4 T along $[110]$ and $[111]$.¹⁵ By means of neutron diffraction, Child *et al.*¹⁷ have determined the field-induced magnetic phase to possess the HoP-type spin structure which is stabilized by tetragonal distortion of DySb. The anomaly

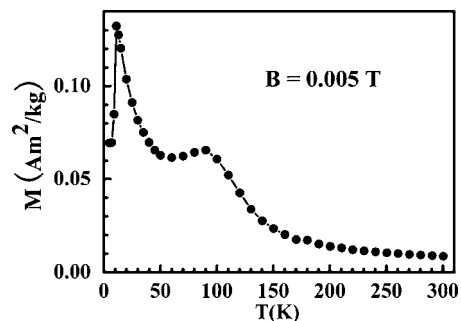


FIG. 1. Temperature dependence of the magnetization of DySb in an external magnetic field of 0.005 T.

^{a)}Electronic mail: wjhu@imr.ac.cn.

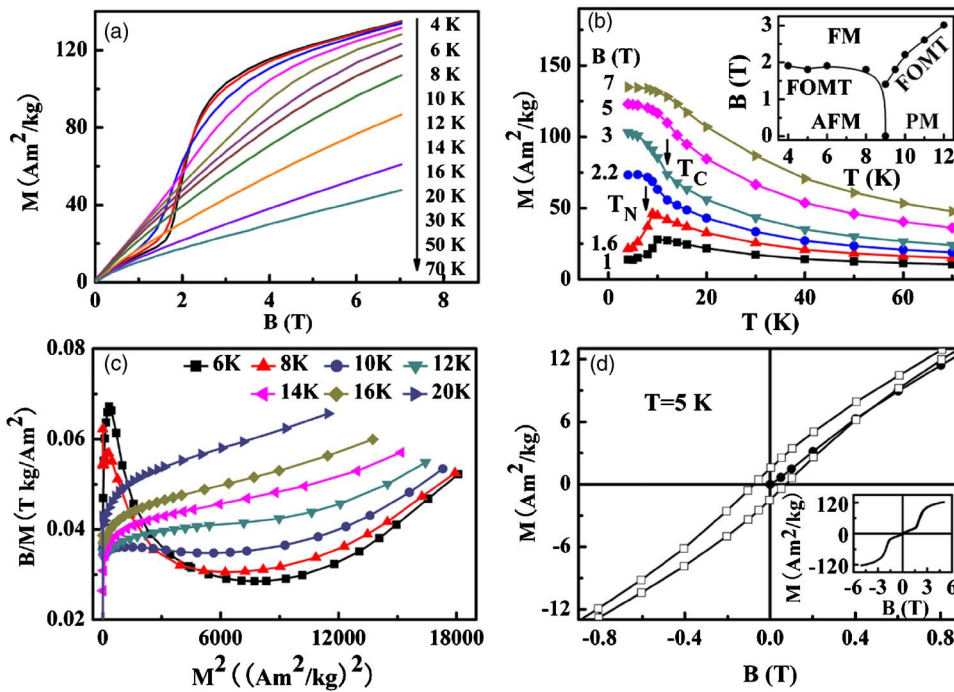


FIG. 2. (Color online) (a) Magnetic-field dependence of the magnetization of DySb at different temperatures. (b) Temperature dependence of the magnetization at different magnetic fields obtained from $M(B)$ data shown in (a). Inset: the magnetic phase diagram of DySb near T_N . (c) Arrott plots at temperatures near T_N . (d) Magnetic-hysteresis curve at 5 K in low magnetic fields. Inset: the hysteresis loop up to 5 T at 5 K.

of magnetization around 90 K may be ascribed to the existence of a minor amount of Dy impurity or to quadrupolar order in the PM region. The latter phenomenon has also been reported for the compound NdSb with the same structure.¹⁸ Nevertheless, it does not contribute to the MCE at low temperatures.

The magnetization curves of DySb between 4 and 70 K are shown in Fig. 2(a). The increments of temperature are different in different temperature ranges: 2 K for 4–8 and 12–16 K, 1 K for 8–12 K, 4 K for 16–20 K, and 10 K for 20–70 K. Below T_N , the magnetization increases slowly with the magnetic field in the low-field range and then jumps at a critical field, but it is not saturated at 7 T. The step in the magnetization curves indicates a field-induced AFM to FM phase transition at low temperatures. The temperature dependence of the magnetization $M(T)$ at different magnetic fields is plotted in Fig. 2(b). A field-induced metamagnetic transition from AFM to FM states is clearly present below T_N . The critical magnetic field B_c (determined from the maximum of dM/dB) for this magnetic transition is about 2 T. Upon increasing the magnetic field to higher values, $M(T)$ exhibits steplike behavior above T_N , which corresponds to the FM/PM transition.

In order to further understand these magnetic transitions, Arrott plots (B/M versus M^2) at different temperatures are shown in Fig. 2(c). The negative slopes or inflection points in the Arrott plots often indicate a first-order phase transition. This criterion has been used in disorder-order transitions between PM and FM states^{19,20} and in order-order AFM to FM transitions¹⁴ [even FM to FM (Ref. 21)]. Therefore, the negative slope of the Arrott plots in low fields below T_N confirms the first-order AFM to FM transition in the applied magnetic field. The inflection points at relatively high fields above T_N (near 12 K) indicate the first-order nature of the PM to FM transitions, in disagreement with Everett and Streit¹⁶ who assumed the transition to be of higher order. The magnetic hysteresis loop at 5 K is shown in Fig. 2(d). The hysteresis ($B_c=0.075$ T and $M_r=1.5$ Am²/kg) is relatively small, compared to typical GMCE materials (for example, the hysteresis

is about 1 T in Gd₅(Ge_{1-x}Si_x)₄⁵ near its magnetic transition temperature). This small hysteresis is believed to originate from the field-induced FM state at low temperatures, which shows normal ferromagnetism with a remanent magnetization and a coercive field.²² The magnetic phase diagram of DySb, obtained by the analysis above, is plotted in the inset of Fig. 2(b), where the phase boundary is determined by the maximum of dM/dB at different temperatures. It will help us to understand the unique MCE of this compound.

The isothermal entropy change, corresponding to a magnetic-field change (ΔB) starting from zero field, was derived from the magnetization data by means of following expression that can be obtained from the Maxwell relation,

$$\Delta S_M(T, B) = S(T, B) - S(T, 0) = \int_0^B \left(\frac{\partial M}{\partial T} \right)_B dB.$$

The curves of $-\Delta S_M$ versus T , shown in Fig. 3, provide with valuable information about the nature of the magnetic ordering in DySb. Here, for small magnetic-field changes, $-\Delta S_M$ is negative (inverse MCE) below T_N , but it changes to small positive values with the increasing temperature, corresponding to the magnetic transition from AFM to PM states

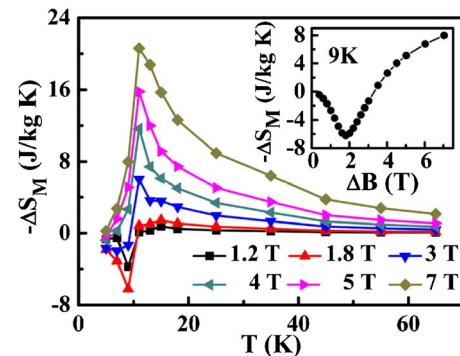


FIG. 3. (Color online) The negative magnetic-entropy change ($-\Delta S_M$) of DySb as a function of temperature for different magnetic-field changes (ΔB). Inset: $-\Delta S_M$ as a function of ΔB at 9 K.

[see the inset of Fig. 2(b)]. The inverse MCE has been often observed in systems displaying first-order magnetic transitions such as AFM/FM [FeRh (Ref. 23)], AFM/FI [Mn_{1.96}Cr_{0.05}Sb (Ref. 24)] or collinear AFM/triangular AFM [ϵ -(Mn_{0.83}Fe_{0.17})_{3.25}Ge (Ref. 13)]. Although the inverse MCE has been seldom reported for a AFM/PM transition, as in the present case, the origin is the same for all of them. Due to the presence of mixed exchange interactions, the applied magnetic field leads to a further spin-disordered state near the transition temperature, increasing the configurational entropy.¹² However, for larger magnetic field changes ($\Delta B = 4\text{--}7$ T), a positive cusplike $-\Delta S_M$ (i.e., a conventional MCE) with its peak position at 11 K is observed. This negative ΔS_M is associated with the first-order PM-FM transition above T_N in higher magnetic fields [see also the inset of Fig. 2(b)], because the magnetic moments are better ordered in an applied magnetic field.

The $-\Delta S_M$ versus ΔB curve at 9 K is plotted in the inset of Fig. 3. At this temperature, a minimum value of $-\Delta S_M$ is observed for $\Delta B = 1.8$ T. Since DySb is an AFII-type antiferromagnet, an increase in the applied field will destroy the antiparallel alignment of the Dy spins, increasing the spin disorder in the AFII system which leads to a negative $-\Delta S_M$. Therefore, the absolute value of $-\Delta S_M$ increases with increasing magnetic field. However, the field-induced metamagnetic transition from AFM to FM states at the critical field of about 1.8 T decreases the absolute value of $-\Delta S_M$ and, at last, changes the sign of $-\Delta S_M$ to positive with the further increasing field. Therefore, the field-induced AFM to FM metamagnetic transition is responsible for the conversion from the inverse to the conventional MCE observed in DySb. The maximum value of $-\Delta S_M$ for DySb (15.8 J/kg K at 11 K for $\Delta B = 5$ T) is comparable to the value reported for the antiferromagnet ErRu₂Si₂ (Ref. 14) (17.6 J/kg K at 5.5 K for $\Delta B = 5$ T), which exhibits the GMCE in the same temperature range.

In summary, both the inverse and the conventional MCE have been observed in the compound DySb. The field-induced MCE conversion at/below T_N is found to be related with the field-induced FOMT from the AFM to the FM states. The giant negative magnetic-entropy change ΔS_M in higher magnetic fields above T_N is associated with the FOMT from the PM to the FM states. The large value of $-\Delta S_M$ (20.6 J/kg K at 11 K for $\Delta B = 7$ T), together with the

small hysteresis suggests that DySb may be a promising candidate to be applied in magnetic refrigeration in the low-temperature range.

This work has been supported by the National Natural Science Foundation of China under Grant No. 50331030.

- ¹K. A. Gschneidner, Jr., V. K. Pecharsky, and A. O. Tsokol, *Rep. Prog. Phys.* **68**, 1479 (2005).
- ²C. B. Zimm, A. Jastrab, A. Sternberg, V. K. Pecharsky, K. A. Gschneidner, Jr., M. Osborne, and I. Anderson, *Adv. Cryog. Eng.* **43**, 1759 (1998).
- ³J. Glanz, *Science* **279**, 2045 (1998).
- ⁴J. A. Barclay and W. A. Steyert, *Cryogenics* **22**, 73 (1982).
- ⁵V. K. Pecharsky and K. A. Gschneidner, Jr., *Phys. Rev. Lett.* **78**, 4494 (1997).
- ⁶F. X. Hu, B. G. Shen, J. R. Sun, Z. H. Cheng, G. H. Rao, and X. X. Zhang, *Appl. Phys. Lett.* **78**, 3675 (2001).
- ⁷H. Wada and Y. Tanabe, *Appl. Phys. Lett.* **79**, 3302 (2001).
- ⁸O. Tegus, E. Brück, K. H. J. Buschow, and F. R. de Boer, *Nature (London)* **415**, 150 (2002).
- ⁹S. Gama, A. A. Coelho, A. de Campos, A. M. G. Carvalho, F. C. G. Gandra, P. J. von Ranke, and N. A. de Oliveira, *Phys. Rev. Lett.* **93**, 237202 (2004).
- ¹⁰S. Stadler, M. Khan, J. Mitchell, N. Ali, A. M. Gomes, I. Dubenko, A. Y. Takeuchi, and A. P. Guimarães, *Appl. Phys. Lett.* **88**, 192511 (2006).
- ¹¹J. Du, Q. Zheng, W. J. Ren, W. J. Feng, X. G. Liu, and Z. D. Zhang, *J. Phys. D* **40**, 5523 (2007).
- ¹²T. Krenke, E. Duman, M. Acet, E. F. Wassermann, X. Moya, L. Manosa, and A. Planes, *Nat. Mater.* **4**, 450 (2005).
- ¹³J. Du, W. B. Cui, Q. Zhang, S. Ma, D. K. Xiong, and Z. D. Zhang, *Appl. Phys. Lett.* **90**, 042510 (2007).
- ¹⁴T. Samanta, I. Das, and S. Banerjee, *Appl. Phys. Lett.* **91**, 152506 (2007).
- ¹⁵R. R. Birss and V. J. Folen, *J. Appl. Phys.* **39**, 1334 (1968).
- ¹⁶G. E. Everett and P. Streit, *J. Magn. Magn. Mater.* **277**, 12 (1979).
- ¹⁷H. R. Child, M. K. Wilkinson, J. W. Cable, W. C. Kockler, and E. O. Wollan, *Phys. Rev.* **131**, 922 (1963).
- ¹⁸E. J. R. Plaza, C. S. Alves, A. A. Coelho, S. Gama, and P. J. von Ranke, *J. Magn. Magn. Mater.* **272**, 2373 (2004).
- ¹⁹H. Saito, T. Yokoyama, and K. Fukamichi, *J. Phys.: Condens. Matter* **9**, 9333 (1997).
- ²⁰K. M. Gu, J. Q. Li, W. Q. Ao, Y. X. Jian, and J. N. Tang, *J. Alloys Compd.* **441**, 39 (2007).
- ²¹X. Z. Zhou, W. L. H. P. Kunkel, and G. Williams, *Phys. Rev. B* **73**, 012412 (2006).
- ²²S. M. Yusuf, M. D. Mukadam, P. Raj, A. Sathyamoorthy, and S. K. Malik, *Physica B* **359**, 1009 (2005).
- ²³M. P. Annaorazov, S. A. Nikitin, A. L. Tyurin, K. A. Asatryan, and A. K. Dovletov, *J. Appl. Phys.* **79**, 1689 (1996).
- ²⁴O. Tegus, E. Brück, L. Zhang Dagula, K. H. J. Buschow, and F. R. de Boer, *Physica B* **319**, 174 (2002).